

Monitoring Spatio-temporal Dynamics of Photosynthesis with a Portable Hyperspectral Imaging System

Uwe Rascher, Caroline J. Nichol, Christopher Small, and Leif Hendricks

Abstract

Photosynthetic efficiency of higher plants dynamically adapts to changing light intensity and is greatly influenced by stress, such as water stress. We tested a new portable hyperspectral imaging system, the SOC-700, manufactured by Surface Optics, which produces 12-bit reflectance images between 440 nm and 880 nm with a 4 nm spectral resolution. We quantified the reflectance properties and photochemical reflectance index (PRI) during light adaptation of genetically modified *Arabidopsis thaliana* (L.) Heynh. plants lacking or over-expressing the PsbS protein, an essential component of the mechanism of non-photochemical dissipation. In a second experiment, PRI images of gradually water stressed leaves were compared to leaf-level measurements of reflectance using a second commercially available spectrometer, and chlorophyll fluorescence to detect dynamic, photosynthesis correlated changes in reflectance and PRI.

In both experiments PRI measured with the SOC-700 changed, reflecting the biochemical adaptation of the photosynthetic apparatus to high light intensity (dynamic changes within minutes) and the gradual deactivation of photosynthesis during drying (changes within hours). The quantum efficiency of photosystem II ($\Delta F/F_m'$) and non-photochemical energy dissipation (NPQ) measured from chlorophyll fluorescence, were strongly correlated with PRI. Leaf area PRI values estimated from individual pixel spectra of the SOC-700 quantified photosynthetic efficiency more thoroughly than PRI values calculated from point measurements using the hand-held GER-1500. The applications, limitations, and potential of the SOC-700 for plant eco-physiology and remote sensing are also discussed.

Introduction

Life on Earth depends on photosynthetic light capture and conversion of this energy to carbohydrates in both marine

phytoplankton and terrestrial plants. Environmental conditions, primarily light intensity, and stress factors such as drought, temperature, or nutrition limitation affect the efficiency of photosynthesis by influencing the biosynthesis, molecular assembly, and functional coordination between molecular components of the photosynthetic apparatus (Schulze and Caldwell, 1996). Excessive absorption of photosynthetic photon fluxes leads to an over-energetization at photosystem II of the photosynthetic apparatus. In order to avoid damage to various biophysical and biochemical mechanisms, non-photochemical energy dissipation processes (NPQ) have evolved in higher plants, regulating the light harvesting and non-photochemical energy dissipation of excessive electrons (see Barber and Andersson, 1992; Krause and Weis, 1991; Schreiber *et al.*, 1995). The main biochemical process for non-photochemical energy dissipation operates as the result of the formation of zeaxanthin, which is the constituent of the so-called xanthophyll cycle. Excess electrons from photosystem II are reduced as the result of de-epoxidation of two pigments, violaxanthin, and antheraxanthin, while the accumulation of zeaxanthin serves as a quantitative indicator for non-photochemical energy dissipation (Demmig-Adams and Adams, 1992; Demmig *et al.*, 1987; Horton *et al.*, 1996; Li *et al.*, 2000). The PsbS protein is an intrinsic pigment-binding photosystem II subunit and directly affects the non-photochemical energy dissipation as the result of the xanthophyll cycle. Even though the exact biochemical and biophysical mechanisms of this process are still under debate, it was shown that maximum NPQ values at high light intensities are greatly decreased in *Arabidopsis thaliana* (L.) Heynh. mutants which have a genetic deficiency of the PsbS protein. Vice versa, *Arabidopsis* plants over-expressing the PsbS protein showed increased NPQ values (Li *et al.*, 2002).

It has been shown that changes in photosynthesis due to drought vary within tropical tree species (Rascher *et al.*, 2004). Therefore, four tropical species were chosen for this study: *Pterocarpus indicus* Willd., *Ceiba pentandra* L., *Pachira aquatica* Aubl., and *Inga cf. sapindoides* Willd., expecting that each species would exhibit a different response to drought conditions, and that each would have its own characteristic time kinetics for drought-induced reduction of photosynthetic efficiency ($\Delta F/F_m'$) and non-photochemical energy dissipation (NPQ).

Uwe Rascher is with the Biosphere 2 Center, Columbia University, P.O. Box 689, Oracle, AZ 85623 and the Institute of Chemistry and Dynamics of the Geosphere ICG-III: Phytosphere, Forschungszentrum Jülich, Stettenericher Forst, 52425 Jülich, Germany (u.rascher@fz-juelich.de).

Caroline J. Nichol is with the Biosphere 2 Center, Columbia University, P.O. Box 689, Oracle, AZ 85623 and the School of GeoSciences, University of Edinburgh, Mayfield Road, Edinburgh, EH9 3JU Scotland, UK.

Christopher Small is at the Lamont Doherty Earth Observatory of Columbia University, Palisades, NY 10964.

Leif Hendricks is at the Surface Optics Corporation, 11555 Rancho Bernardo Rd., San Diego, CA 92127.

Photogrammetric Engineering & Remote Sensing
Vol. 73, No. 1, January 2007, pp. 045–056.

0099-1112/07/7301-0045/\$3.00/0
© 2007 American Society for Photogrammetry
and Remote Sensing

One of the most powerful tools to measure leaf photosynthetic efficiency, electron transport, and non-photochemical energy dissipation processes is the non-invasive quantification of the fluorescence signal of chlorophyll *a* of photosystem II (Schreiber and Bilger, 1993; Schreiber *et al.*, 1995; Maxwell and Johnson, 2000). Quantum yield of photosystem II, either measured in the dark adapted state (potential quantum yield: F_v/F_m) or in the light adapted state (effective quantum yield: $\Delta F/F_m'$), as well as non-photochemical quenching (NPQ), which accounts for the sum of all non-photochemical energy dissipating processes, are proven to be robust parameters for quantifying leaf photosynthesis (Maxwell and Johnson, 2000). Fully developed, non-stressed leaves of higher plants reveal F_v/F_m values of 0.83 after a dark period of several hours (Bradbury and Baker, 1981). Any drop of this predawn value below 0.80 can be considered as an indication of a substantial limitation in electron flow or photoinhibition. $\Delta F/F_m'$ and NPQ values dynamically adapt primarily to changes in light intensity, however if irradiance is kept constant those parameters reflect the underlying mechanisms, such as light stress induced activation of the xanthophyll cycle (Demmig *et al.*, 1987; Bassi and Caffari, 2000), drought stress (Griew *et al.*, 1995; Valentini *et al.*, 1995), or severe substrate limitation (Thornley, 1998). In order to obtain these parameters, photosynthesis has to be excited actively by e.g., a saturating light pulse, which still limits this method for remote ecosystem monitoring. Laser-induced spot- or scanning-methods (Kolber *et al.*, 1998, 2005; Ananyev *et al.*, 2005) or narrow waveband measurements in the Fraunhofer lines (Carter *et al.*, 1996) may overcome this methodological difficulty in the future.

Hyperspectral reflectance measurements show increasing potential for monitoring plant ecosystems. The Photochemical Reflectance Index (PRI) was developed to serve as an estimate of photosynthetic light use efficiency (Gamon *et al.*, 1993; 1997; Peñuelas *et al.*, 1995a) and can be derived from hyperspectral reflectance measurements. This normalized difference reflectance index uses two wavebands: 531 nm, which is affected by the de-epoxidation of violaxanthin to zeaxanthin, and 570 nm, which remains unaffected by the de-epoxidation reaction (Gamon *et al.*, 1992). The PRI positively correlates with photosynthetic efficiency, is negatively correlated with NPQ and has been successfully used to detect changes in photosynthetic efficiency at the leaf level (Peñuelas *et al.*, 1995b and 1997; Gamon *et al.*, 1997; Guo and Trotter, 2004), small canopy level (Gamon *et al.*, 1992; Filella *et al.*, 1996; Styliński *et al.*, 2002; Trotter *et al.*, 2002), and recently at the ecosystem level (Peñuelas and Inoue, 2000; Rahman *et al.*, 2001; Nichol *et al.*, 2000 and 2002). However, absolute PRI values vary greatly between species with the same photosynthetic capacity (Guo and Trotter, 2004), and were greatly affected by seasonal changes in canopy structure (Filella *et al.*, 2004). Generally, as the scale moves up from the leaves to canopies, the relationships vary, and if used with low precision filters, ecosystem measurements of PRI have failed to predict photosynthetic efficiency (Methy, 2000). Nevertheless, PRI still remains as the only valid reflectance index directly implicated in the photosynthetic reactions.

It is known that photosynthetic efficiency is not homogeneously distributed over leaves and may show spatial and temporal variations (Rascher, 2003). For example, spatial heterogeneity of photosynthetic activity is shown to occur in variegated *Abutilon striatum* leaves (Osmond *et al.*, 1998) in optically, uniformly green leaves during wilting (Osmond *et al.*, 1999), during crassulacean acid metabolism (CAM) mode of photosynthesis (Rascher and Lüttge, 2002; Rascher *et al.*, 2001), and during leaf development (Walter *et al.*, 2004). Three-dimensional canopies, which are complex

assemblages of leaves and individual plants, are even more complicated and photosynthetic efficiency greatly fluctuates in time and space (Frak *et al.*, 2002). Modeling studies show that PRI was strongly influenced by canopy structure, view, and illumination angles (Barton and North, 2000). Additionally, PRI might be affected by the ratio of chlorophyll and carotenoids and cell morphological changes, which complicates inter-species comparisons of absolute values. Spatially explicit imaging systems are needed to elucidate the complex spatial properties of single leaves and natural ecosystems and to scale leaf-level to ecosystem responses, which was recently emphasized in the context of global climate change (National Academies, 2004) and remains a challenge for future ecosystem research (Enquist *et al.*, 2003).

Materials and Methods

Plants

Light induction kinetics were performed using the wild-type, and the mutants L5 (PsbS protein over expressed), and npq4-1 (PsbS protein absent) of *Arabidopsis thaliana* (L.) Heynh. (ecotype Col-0; Li *et al.*, 2002). The pigment-binding PsbS protein of the small subunit of the light-harvesting complex directly affects the non-photochemical energy dissipation as a result of the xanthophyll cycle. Single plants of wild type and mutants (maintained in a growth chamber at $100 \mu\text{mol photons m}^{-2} \text{s}^{-1}$) were dark adapted for 30 minutes prior to exposures to sunlight (Photon Flux Density) (PFD) = $1,300 \mu\text{mol photons m}^{-2} \text{s}^{-1}$), and then measured for 25 minutes (1 to 5 minute intervals).

Leaves from four tropical trees, namely *Pterocarpus indicus* Willd., *Ceiba pentandra* L., *Pachira aquatica* Aubl., and *Inga cf. sapindoides* Willd., from inside the Biosphere 2 Center, Oracle, Arizona, were detached in the early morning and fixed on a cardboard under dim light (PFD < $1 \mu\text{mol m}^{-2} \text{s}^{-1}$) using super-glue on the veins only (CN-polymer). The cardboard was then placed on the wall of an air-conditioned room at constant temperature and humidity (20°C and 60 percent RH). Leaves were dark adapted for 15 minutes after assembly, and then light (PFD = 160 to $190 \mu\text{mol m}^{-2} \text{s}^{-1}$) was provided by a 600 watts tungsten lamp (AL 1000, Arrilite, Germany) and was monitored throughout the experiment. PFD was homogeneously distributed with a slight (15 percent) decrease towards the edges of the board. Leaves were subjected to drying under these constant conditions and measurements were taken just before and after the onset of light and then every 30 minutes.

A calibrated reflectance panel (Spectralon, Labsphere, North Sutton, New Hampshire) was placed within the field of view (see Figure 1, lower left corner of each frame) to allow normalization of radiance values to reflectance.

Chlorophyll Fluorescence Measurements

The chlorophyll *a* fluorescence measurements were performed with the miniaturized pulse-amplitude modulated photosynthesis yield analyzer (Mini-PAM) of H. Walz (Effeltrich, Germany) with the leaf clip holder described by Bilger *et al.* (1995). The effective quantum yield of photosystem II ($\Delta F/F_m'$) was calculated as $(F_m' - F)/F_m'$ (Genty *et al.*, 1989), where F is fluorescence yield of the light adapted sample and F_m' is the maximum light-adapted fluorescence yield when a saturating light pulse of 800 ms duration (intensity approximately $3000 \mu\text{mol m}^{-2} \text{s}^{-1}$) is superimposed on the prevailing environmental light levels (Schreiber and Bilger, 1993). Potential quantum yield of photosystem II (F_v/F_m) was measured before the onset of light and during the light period of the experiment using the leaf clips of H. Walz, with which small patches of the leaves

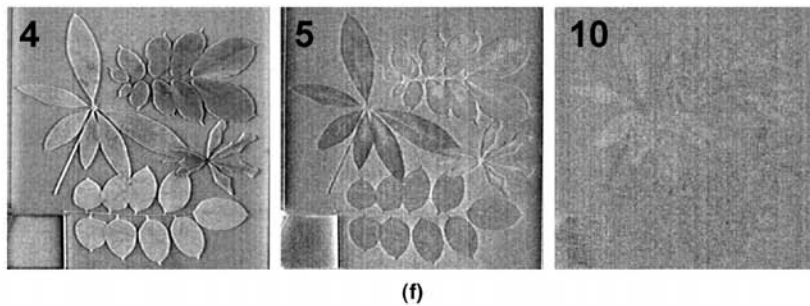
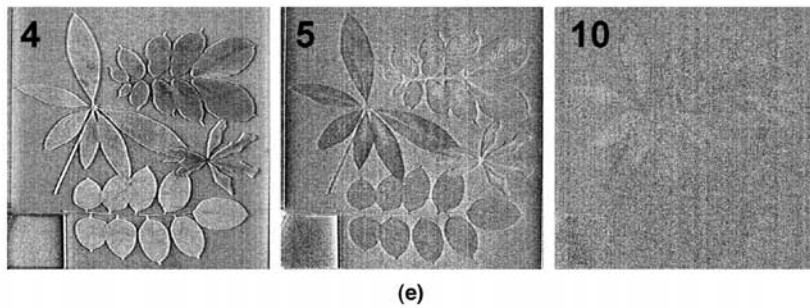
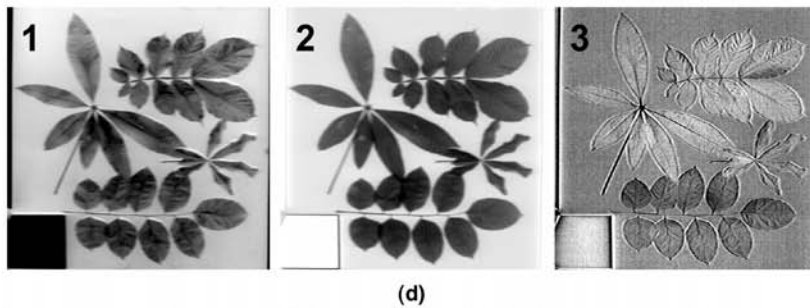
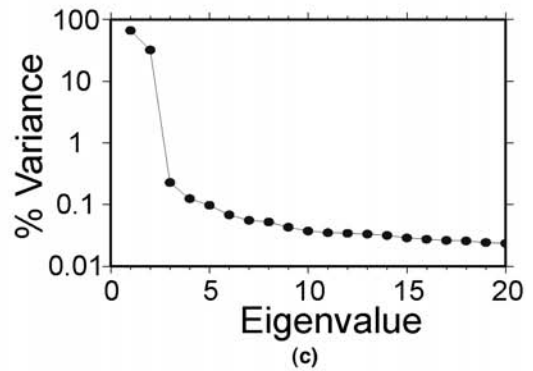
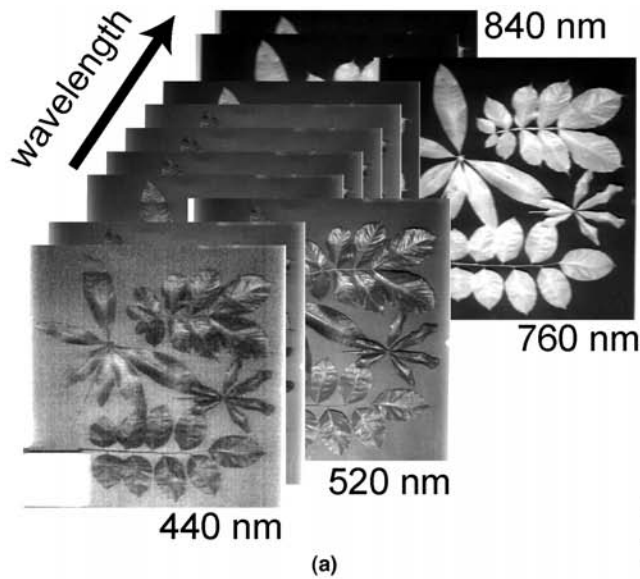


Figure 1. Transformation and filtering procedure of the hyperspectral imaging cubes obtained with the SOC-700 field portable hyperspectral reflectometer: (a) Example of a hyperspectral cube, (b) The SOC-700 reflectometer, which can be controlled by a notebook or desktop computer, (c) Eigenvalues and the variance of the Principle Component (PC) vectors, (d and e) PC vectors of the reflectance cubes after the MNF transformation: no filter applied (The numbers indicate the number of the PC vector.) and (f) PC vectors after filtering with a low pass Gaussian filter, which was applied over an 11 pixel \times 11 pixel area.

were dark adapted for 15 minutes. Non-photochemical processes, i.e., non-photochemical quenching (NPQ), were calculated as $(F_m - F_m')/F_m'$ (Bilger and Björkman, 1990). Prior and just after each measurement run, a fluorescence standard was measured to account for the different sensitivity of the instrument. Absolute values were corrected using these standard measurements.

Hyperspectral Reflectance Spot Measurements Using the GER-1500

Leaf reflectance for the four species was measured using a GER-1500 (Spectra Vista Corp, Poughkeepsie, New York). The GER-1500 has a useable spectral range from 350 nm to 1,050 nm with 512 spectral bands. The Full Width at Half Maximum (FWHM) of the GER-1500 is 3 nm. Reflectance measurements were taken from a distance of 30 cm for each leaf using the 4° lens barrel for a leaf area of approximately 4 cm diameter. Reflectances were calculated by normalizing the leaf radiance by the radiance of a 99 percent calibrated reflectance standard (Spectralon, Labsphere, North Sutton, New Hampshire), which was measured immediately before each leaf measurement.

Hyperspectral Imaging of Reflectance Using the SOC-700

Hyperspectral images were acquired using the SOC-700 (Surface Optics, Corp., San Diego, California; Figure 1b). Images have 640 pixels × 640 pixels and a spectral resolution of approximately 4 nm with 120 equally distributed bands in the range of 400 to 900 nm (Figure 1). The FWHM varies slightly with wavelength, but on average is 4.55 nm providing a minimum overlap of approximately 18 percent. The imager is a line-scanning push broom configuration. Light enters the instrument through the front aperture, travels through a pair of folding mirrors (one of which rotates to provide scanning) and enters the optical system through a C-mount lens (Schneider Xenoplan 1.9/35 mm.). The lens images a column of data on to a horizontal slit at the entrance of the imaging spectrometer. The slit width (25 microns) determines the spectral resolution of the instrument as well as its light gathering capability. The imaging spectrometer is an ImSpector V9 (www.specim.fi) composed of the entrance slit, fore-optics, a prism-grating-prism spectrometer and some additional exit optics. The diffraction grating is of holographic design with an efficiency of approximately 50 percent over the entire spectral range. A row of imaged points is spread out spectrally along the y-axis and then imaged on to a 640 pixel × 480 pixel silicon CCD array, with a 12-bit dynamic range (PCO AG, Kelheim, Germany). The data are binned by 4 in the y-dimension to improve the signal to noise ratio resulting in a row of data, which is 640 pixels wide and 120 bands deep. Data are recorded for 640 scans and stored as 16-bit unsigned integer image cubes 640 × 640 × 120 pixels in extent. The first two dimensions are the spatial size of the image, and the third dimension is the spectral. A single cube requires approximately 98 MB of storage space and can be processed and analyzed using the SOC software HS-Analysis or other hyperspectral processing packages, such as ENVI software.

The instrument yields absolute radiometric values as well as relative reflectance if a suitable standard is present in the image for calibration or precise information is available regarding scene irradiance. SOC's HS-Analysis software compensates for the 700's *spectral smile*. Spectral smile is the slight deviation in wavelength as one reaches the edges of the spatial dimension and is characteristic of this type of imaging spectrometer. Dark noise compensation requires that prior to each measurement series, a dark image be obtained to account for the inherent dark noise in the detector and electronics which varies with exposure time and ambient

temperature. Dark images are obtained in the SOC-700 by rotating the scan mirror until it is facing the spectrometer creating a dark path for imaging.

Data Analyses

Hyperspectral cubes obtained with the SOC-700 were linearly corrected using the dark image, acquired prior to each measurement, and normalized to the 99 percent calibrated reflectance standard (Spectralon, Labsphere, North Sutton, New Hampshire) using the HS-Analysis Software provided with the SOC-700. All further analyses were performed using the reflectance images.

Images were filtered in Principal Component space as described by Green *et al.*, 1988 (Figure 1c through 1f) using the ENVI 3.5 software package (Research Systems, Inc., 2000). The filtering procedure is described in the results section in detail.

The Normalized Difference Vegetation Index (NDVI) and Photochemical Reflectance Index (PRI; Gamon *et al.*, 1992) were calculated according to Equations 1 and 2, respectively:

$$NDVI = \frac{R_{780} - R_{670}}{R_{780} + R_{670}} \quad (1)$$

$$PRI = \frac{R_{531} - R_{570}}{R_{531} + R_{570}} \quad (2)$$

where $R_{\text{wavelength}}$ indicates the reflectance at this wavelength.

The GER-1500 provides reflectance measurements at exactly these wavelengths, which were used for the calculation of PRI. Single wavebands of the SOC-700 imaging system were approximately 4 nm apart; thus, wavelengths may not exactly meet the definition for PRI and may vary slightly with the single instrument calibration. We used the reflectance at the closest wavelength available, which in our case were 532.4 nm and 569.0 nm for the drying experiment, and 530.5 nm and 571.6 nm for the measurements of *Arabidopsis thaliana* (L.) Heynh. The PRI was then calculated using pixel arithmetic. Mean values for one leaf were obtained by manually selecting a region of interest, which covered all leaf area, excluding the middle rip and the very edge of the leaf. We are aware that our data sets were not normally distributed, and we thus computed correlation between the PRI and fluorescence yield and between PRI values obtained by different instruments using non-parametric rank correlations according to Spearman (SAS Software Packet, SAS Institute, Inc., Cary, North Carolina).

Results

Hyperspectral Imaging Data

Radiance images from the SOC-700 were normalized using the reflectance standard provided in the lower left corner of each image (Figure 1 and Plate 2). The hyperspectral reflectance images of the leaves show the characteristic spectra of living plant material (Figure 2). However, data at the extremes of the spectral range of the instrument appeared to be noisy, and thus, were not used in the analyses. These data are captured at the edge of the spectral response curves for silicon, the material used in the CCD, where efficiency is lowest and did not provide adequate signal to noise ratio.

Principal Component Analyses and Data Filtering

Principal component analysis suggests that the SOC-700 provides sufficient spectral redundancy to allow noise

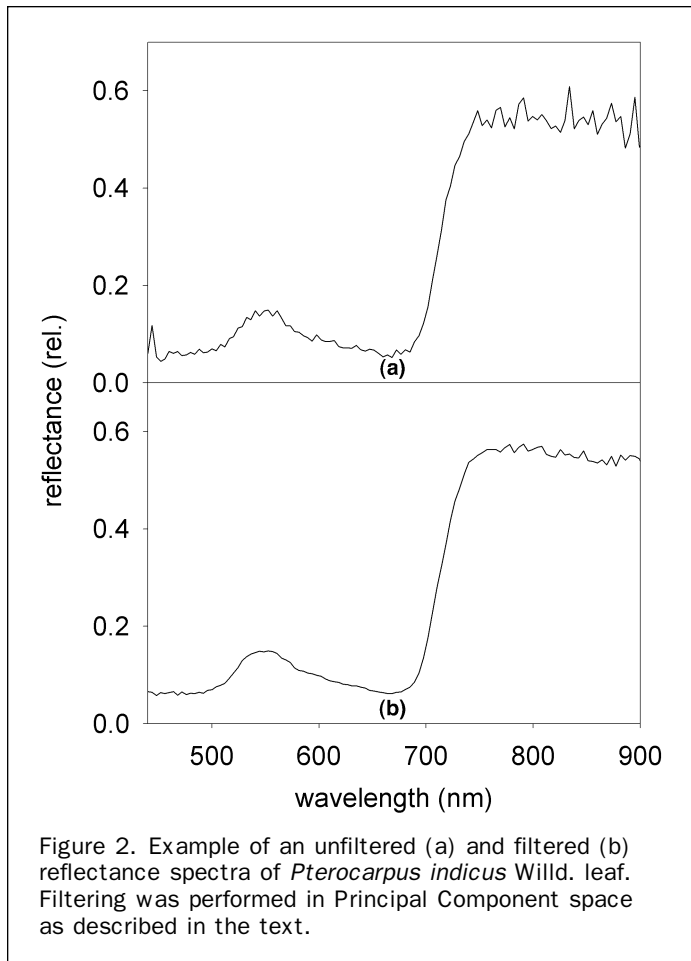


Figure 2. Example of an unfiltered (a) and filtered (b) reflectance spectra of *Pterocarpus indicus* Willd. leaf. Filtering was performed in Principal Component space as described in the text.

reduction by smoothing the high order Principal Components (PC). A Minimum Noise Fraction (MNF) transformation (Green *et al.*, 1988) was used to obtain the principal components and estimate spectral dimensionality. The MNF transformation implemented in ENVI is analogous to the Maximum Noise Transformation described by Green *et al.* (1988) but differs in ordering of the principal components from high to low signal variance (Research Systems, Inc., 2000). The MNF transformation is similar to a covariance-based PC transformation, but offers the added benefit of normalizing the Eigenvalues relative to the variance of the sensor noise estimate so that noise in high amplitude bands does not outweigh signal in lower amplitude bands. For this analysis, all MNF transformations were applied using noise covariance statistics derived from the corresponding dark image of the series. In this transformation, spectral cubes were transformed to PC images (Figure 1d and 1e), where each image is associated with an eigenvalue (Figure 1c), which gives the variance associated with that PC image. PC vectors 1 to 3 contain most (98.7 percent) of the variance and were left unfiltered, as noise was negligible in these vectors (Figure 1d). PC vectors of higher order (4 to 120; Figure 1e) showed greater noise levels; however, spatial information was clearly visible in images 4 to 12. In order to reduce the pixel-to-pixel variations, we convolved each PC image with a low-pass Gaussian kernel of 11 pixels \times 11 pixels (Figure 1f). After filtering the high order PC images, the cubes were reconstructed using unfiltered PC vectors 1 to 3 and filtered PC vectors 4 to 120. Inverse MNF transformation yielded the original hyperspectral image cubes with a clearly reduced noise level and smoother spectra (Figure 2). PC

vectors of *Arabidopsis thaliana* (L.) Heynh. were filtered in three categories: PC vectors 1 to 3 were left unfiltered, PC vectors 4 and 5 were filtered with a 5 pixel \times 5 pixel low-pass Gaussian kernel, and PC vectors 6 to 120 were filtered with a 11 \times 11 kernel.

Images of PRI were calculated using pixel arithmetic. PRI values of leaves were per definition close to zero, and thus, leaf values were hard to distinguish from the background (Plate 2D). Therefore, pictures were masked using the NDVI, as a selective parameter to separate green leaf material from the background (Plate 2B). PRI images, which were masked with the NDVI threshold image (Plate 2C), produced spatially clearly conceivable images of each leaf (Plate 1 and Plate 2E through 2H).

Light Induction of Photosynthesis

Light reaction of photosynthesis adapts to exposure to high light intensity and non-photochemical energy dissipation processes gradually increase within minutes and are known to saturate. Levels of saturation are increased for the L5 mutant and greatly decreased for the npq4 mutant (Li *et al.* 2000 and 2002). PRI values of the three *Arabidopsis thaliana* (L.) Heynh. strains were different at the beginning of light exposure, with the npq4 mutant having the highest (PRI = -0.033 ± 0.013) and the L5 mutant having the lowest absolute value (mean PRI = -0.052 ± 0.017). These differences in PRI can be used to distinguish the three stains of *Arabidopsis thaliana* (L.) Heynh., which are undistinguishable for the bare eye (Plate 1). With time of light exposure, PRI of the wild-type (WT) and the L5 mutant increased and PRI of the npq4 mutant decreased (Figure 3a). We normalized the PRI values to the first value (1 minute after light exposure) in order to show the relative changes of PRI within each strain (Figure 3b). PRI of L5 increased by 6 percent saturating at the highest relative increase during light exposure and PRI of the WT increased by 3 percent. PRI of the npq-4 mutant declined after a short increase during the first five minutes and finally reached a value 6 percent below the initial PRI.

The Effect of Water Stress on Reflectance

First, we investigated the changes in the overall shape of reflectance spectra (from the GER-1500 measurements as this is the commercially available instrument) in visible and near-infrared reflectance by looking at the difference reflectance between the start of the experiment (30 minutes after leaf cutting) and then 1.5, 3.5, and 5.5 hours later, during the drying out phase (Figure 4). With *Pterocarpus indicus* Willd. and *Inga cf. sapindoides* Willd. reflectance increased greatly at 560 nm and within the infrared (Figure 4a and 4c). A similar, even though small, behavior was detected until 4h at *Pachira aquatica* Aubl. (Figure 4b). The increase in visible and decrease in infrared reflectance as seen with *Ceiba pentandra* L. and *Pachira aquatica* Aubl. (Figure 4b and 4d) after 3.5 and 5.5 hours, respectively, is a clear indication of severe dehydration and the associated structural changes within the leaves (Carter and Knapp, 2001).

The Effect of Water Stress on Photosynthesis

The light reaction of photosynthesis was clearly affected by the drying process (Figure 5). Photosynthesis of all four plants showed high potential quantum yield (F_v/F_m) at and above 0.8 before the onset of light, indicating that all leaves were in a healthy state and not photoinhibited. Every two hours, small patches of the leaves were dark adapted for 15 minutes using the dark leaf clips of H. Walz and F_v/F_m was measured (Figure 5A through 5D, closed symbols). The fast recovery of F_v/F_m values of *Pterocarpus indicus* Willd. and *Inga cf.*

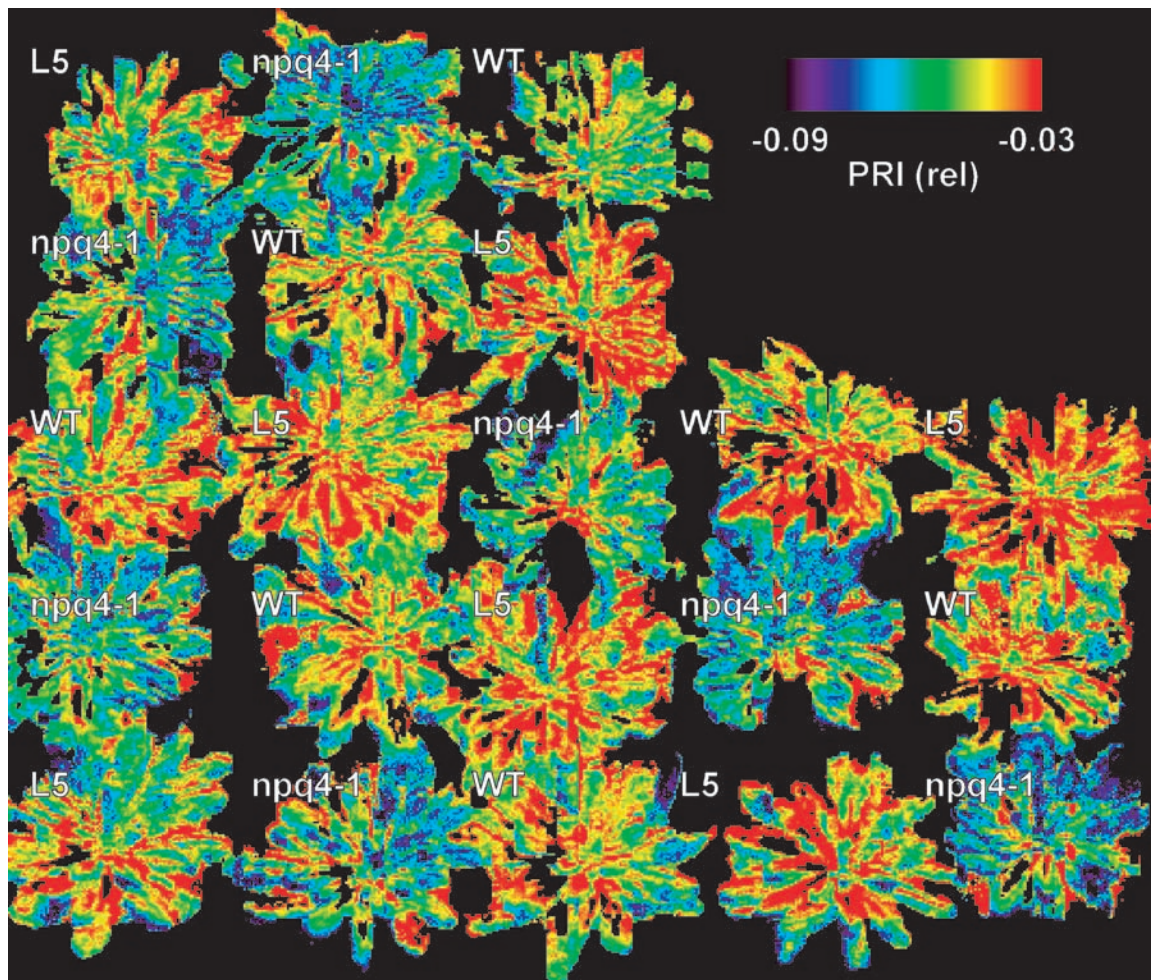
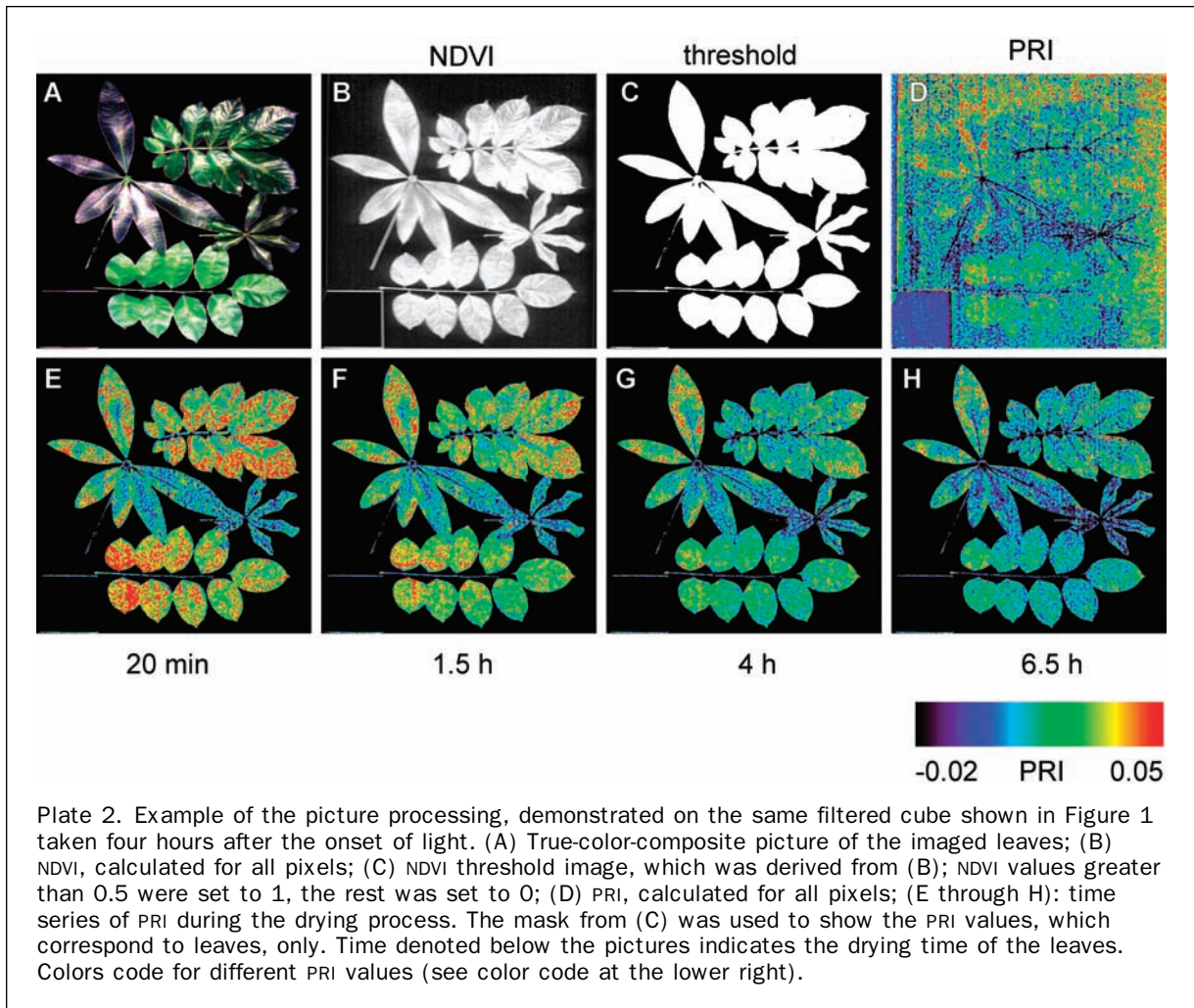


Plate 1. Map of Photochemical Reflectance Index (PRI) of three strains of *Arabidopsis thaliana* (L.) Heynh. after 30 minutes of dark adaptation. PRI was measured just after exposure to sun light (PFD = $1300 \mu\text{mol m}^{-2} \text{s}^{-1}$). The three strains were wildtype (WT), over expressed PsbS protein (L5) or were deficient of PsbS (npq4).

sapindoides Willd. throughout the experiment proved that photosynthetic apparatus of these leaves was in a fully functioning state. F_v/F_m values of *Pachira aquatica* Aubl. decreased below 0.6 6 hours within the experiment and F_v/F_m values of *Ceiba pentandra* L. dropped to zero after 2.2 hours, indicating photodamage (Figure 5B, 5F, and 5J; vertical dashed lines, grey symbols). In the following, we will only refer to the time periods with a physiological functioning photosynthetic apparatus and will ignore photodamaged leaves. At all species, effective quantum yield of the light adapted leaves ($\Delta F/F_m'$) decreased with time to values between 0.2 and 0.4, showing the gradual reduction of photosynthetic efficiency (Figure 5A through 5D; open symbols). However, $\Delta F/F_m'$ of the shade adapted *Pachira aquatica* Aubl. decreased rapidly (within the first 20 minutes) to low values, which then remained constant until photodamage. Non-photochemical energy dissipation, expressed as NPQ, increased within the first hour to maximum values between 2 and 3 at *Pterocarpus indicus* Willd. and *Pachira aquatica* Aubl., NPQ of *Ceiba pentandra* L. and *Inga cf. sapindoides* Willd. saturated at about 1 (Figure 5E through 5H). NPQ values of *Pachira aquatica* Aubl. increased to maximum values within the first 30 minutes after the onset of light and then remained constant, again reflecting the fast adaptation of

photosynthesis of this shade adapted plant to the exposure to relatively high light intensities. NPQ values of all plants dropped to almost zero after 15 minutes of intermittent dark adaptation, indicating that non-photochemical energy dissipating is mediated by dynamic processes such as the xanthophyll cycle (Figure 5E through 5H; closed symbols).

These changes in photosynthetic efficiency using chlorophyll fluorescence were also detected in the PRI (Figure 5I through 5L). Generally, PRI decreased with time of water stress. Additionally, PRI was heterogeneously distributed over the single leaves (Plate 2E through 2H), however, spatial heterogeneity, which was calculated for single leaves using cellular automaton techniques (Hütt and Neff, 2001), did not change significantly during the drying process (personal communication M.T. Hütt, data not shown). Spatial means of PRI of *Pterocarpus indicus* Willd. and *Inga cf. sapindoides* Willd. were highest at the beginning of the experiment and then gradually declined, showing similar time kinetics as $\Delta F/F_m'$ (Figure 5I and 5J). PRI values obtained by the SOC-700 (PRI_{SOC-700}) were consistently lower than those measured with the GER-1500 (PRI_{GER-1500}), and variations occurred in a smaller range. For *Pachira aquatica* Aubl. PRI_{SOC-700} & GER-1500 values slightly declined throughout the drying process with both instruments



delivering comparable trends (Figure 5K). For *Ceiba pentandra* L. $PRI_{SOC-700}$ values remained constant throughout the experiment, with two $PRI_{GER-1500}$ values being greatly offset (Figure 5L).

Correlation Analyses of PRI

The data shown in Figure 5 cannot be considered normally distributed, and as thus, we used the non-parametric rank-correlation according to Spearman to test data for correlation (Table 1). The Spearman rank-coefficient (r_s) is equivalent to the regression correlation coefficient.

$PRI_{SOC-700}$ & $GER-1500$ was positively correlated with $\Delta F/F_m'$ for *Pterocarpus indicus* Willd. and *Inga cf. sapindoides* Willd. Marginal correlations was also obtained for $PRI_{SOC-700}$ for *Pachira aquatica* Aubl., while no correlation could be found between $\Delta F/F_m'$ and the PRI values measured with the GER-1500 for *Ceiba pentandra* L. and *Pachira aquatica* Aubl. $PRI_{SOC-700}$ was negatively correlated with NPQ for *Pterocarpus indicus* Willd. and *Inga cf. sapindoides* Willd. No significant correlation was found between NPQ and the PRI values for *Pachira aquatica* Aubl. or *Ceiba pentandra* L. (Table 1). In general, correlation was better between $PRI_{SOC-700}$ and $\Delta F/F_m'$ than for NPQ. Mean $PRI_{SOC-700}$ values also correlated more closely with $\Delta F/F_m'$ and NPQ than the PRI data measured with the GER-1500.

We directly compared $PRI_{SOC-700}$ and $PRI_{GER-1500}$ values of both instruments across three of the four species (*Pterocarpus indicus* Willd., *Inga cf. sapindoides* Willd., and *Pachira aquatica* Aubl.; Figure 6). Using the results from the three

species, we calculated a general linear transformation to compare PRI data from the two instruments ($r_s^2 = 0.69$) (Equations 3 and 4). However, this regression may depend on the single instrument and its exact wavelengths of detection and, thus has to be adapted for the single use. We did not include *Ceiba pentandra* L. in this analyses as these leaves were physiologically dead after the first two hours, and thus, PRI values did not correlate ($r_s^2 = 0.22$).

$$PRI_{SOC-700} = 0.4753 \cdot PRI_{GER-1500} - 0.0027 \quad (3)$$

$$PRI_{GER-1500} = 2.1039 \cdot PRI_{SOC-700} + 0.0057 \quad (4)$$

Discussion

In this study, we investigated the Photochemical Reflectance Index (PRI) and its relation to quantum yield of photosystem II ($\Delta F/F_m'$) and non-photochemical energy dissipation (NPQ) of *Arabidopsis thaliana* (L.) Heynh. mutants and four tropical plants using a new cost effective hyperspectral imaging device (SOC-700) and a commercially available spectrometer (GER-1500).

With many CCD-based devices, a problem of a low signal to noise ratio can exist. This limited dynamic range was clearly visible in the raw data of the SOC-700 (Figure 2). As a consequence, a filtering procedure was necessary to extract sensitive properties from the reflectance signature. The mode and degree of filtering, as well as any thresholds must

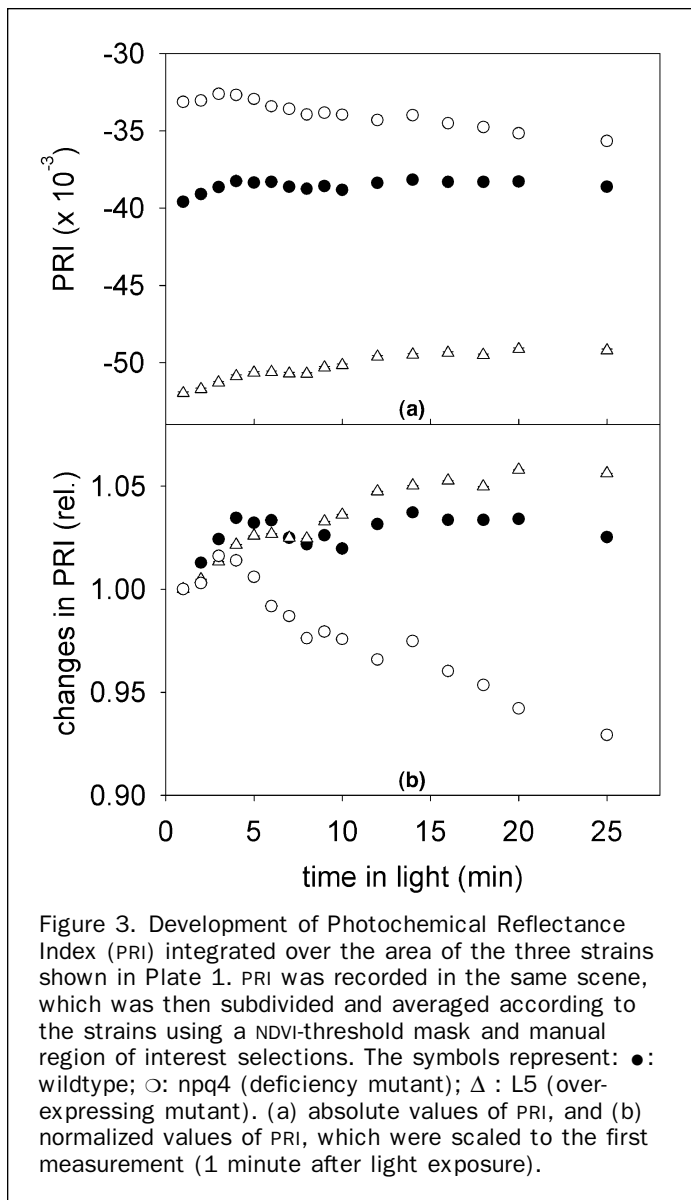


Figure 3. Development of Photochemical Reflectance Index (PRI) integrated over the area of the three strains shown in Plate 1. PRI was recorded in the same scene, which was then subdivided and averaged according to the strains using a NDVI-threshold mask and manual region of interest selections. The symbols represent: ●: wildtype; ○: npq4 (deficiency mutant); △: L5 (over-expressing mutant). (a) absolute values of PRI, and (b) normalized values of PRI, which were scaled to the first measurement (1 minute after light exposure).

be considered a critical point in several respects: (a) fixed thresholds as used in our procedure may introduce hidden artifacts, (b) filtering can be too severe and may eliminate low amplitude signals (in our case study the minimal shift of the reflectance at 531 nm), (c) principal component (PC) transformations are data dependent in the sense that the rotation is determined by the band covariance (For this reason, it is necessary to apply the spatial filtering on the basis of the spatial coherence of the higher order PC images. The combination of the spatial coherence of the PC images and the variance distribution given by the normalized Eigenvalues shows the transition from signal to noise.), and (d) The size of the Gaussian Filter and the number of principle components filtered can be adjusted according to the spatial and spectral structure of the data. We found this procedure to be very robust (not overly sensitive to small changes in filter size or PC bands used) and to yield reproducible results showing the gradual inactivation of photosynthesis, reflected in PRI.

The higher dynamic range of the GER-1500 was complemented by the spatial information obtained by the SOC-700. The mean values of PRI_{SOC-700}, which always took the same

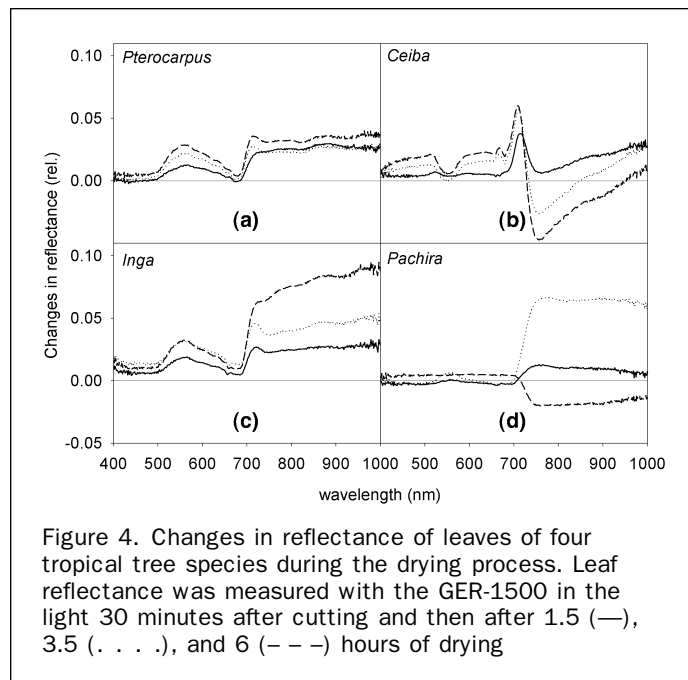


Figure 4. Changes in reflectance of leaves of four tropical tree species during the drying process. Leaf reflectance was measured with the GER-1500 in the light 30 minutes after cutting and then after 1.5 (—), 3.5 (. . .), and 6 (- - -) hours of drying

area of a leaf into account, correlated strongly $\Delta F/F_m'$ and NPQ. Spatial heterogeneity of photosynthesis must be assumed to be an inherent physiological property of leaves (Chaerle and Van der Straeten, 2001; Meyer and Genty, 1998; Osmond and Park, 2001; Rascher, 2003; Rascher and Lüttge, 2002) particularly during water stress and wilting when pronounced heterogeneity of photosynthetic efficiency has been reported (Meyer and Genty, 1999; Osmond *et al.*, 1999). From the data presented here, spatial variations of PRI may be based on physiological heterogeneity of photosynthesis on the one hand and locally different absorption and reflection properties because of non-uniform surface structures and wrinkling on the other hand.

Generally, leaf reflectance in the visible light is dominated by pigment absorption, while reflectance in the near-infrared reflects structural properties of leaves (Carter and Knapp, 2001; Richardson and Berlyn, 2002). We assume that during the hour-long drying experiment with the tropical leaves both effects may contribute to changes in reflectance (Figure 4). Changes in PRI most likely reflect underlying changes in the xanthophyll cycle; however, we cannot totally exclude the possibility that structural changes during the drying process may also have affected PRI in this experimental run. Those species dependent differences can be excluded for the measurements with the anatomically and structurally identically *Arabidopsis thaliana* (L.) Heynh. plants. The changes of PRI, which were detected within a few minutes during light adaptation of the *Arabidopsis thaliana* (L.) Heynh. mutants, are not due to structural changes but certainly reflect the gradual activation of NPQ as a result of the xanthophylls cycle as a response to excessive light. The results with *Arabidopsis* mutants are quantitatively and kinetically similar to those obtained using PAM (Li *et al.*, 2002) and other fluorescence techniques (Kolber *et al.*, 2005). They confirm interpretations of the components of NPQ associated with the levels of expression of the ΔpH sensing small protein subunit PsbS in the super complex of PSII. We thus also conclude that the PRI recorded with this new hyperspectral imaging instrument can be used to quantify dynamic, biochemical changes of photosynthetic efficiency.

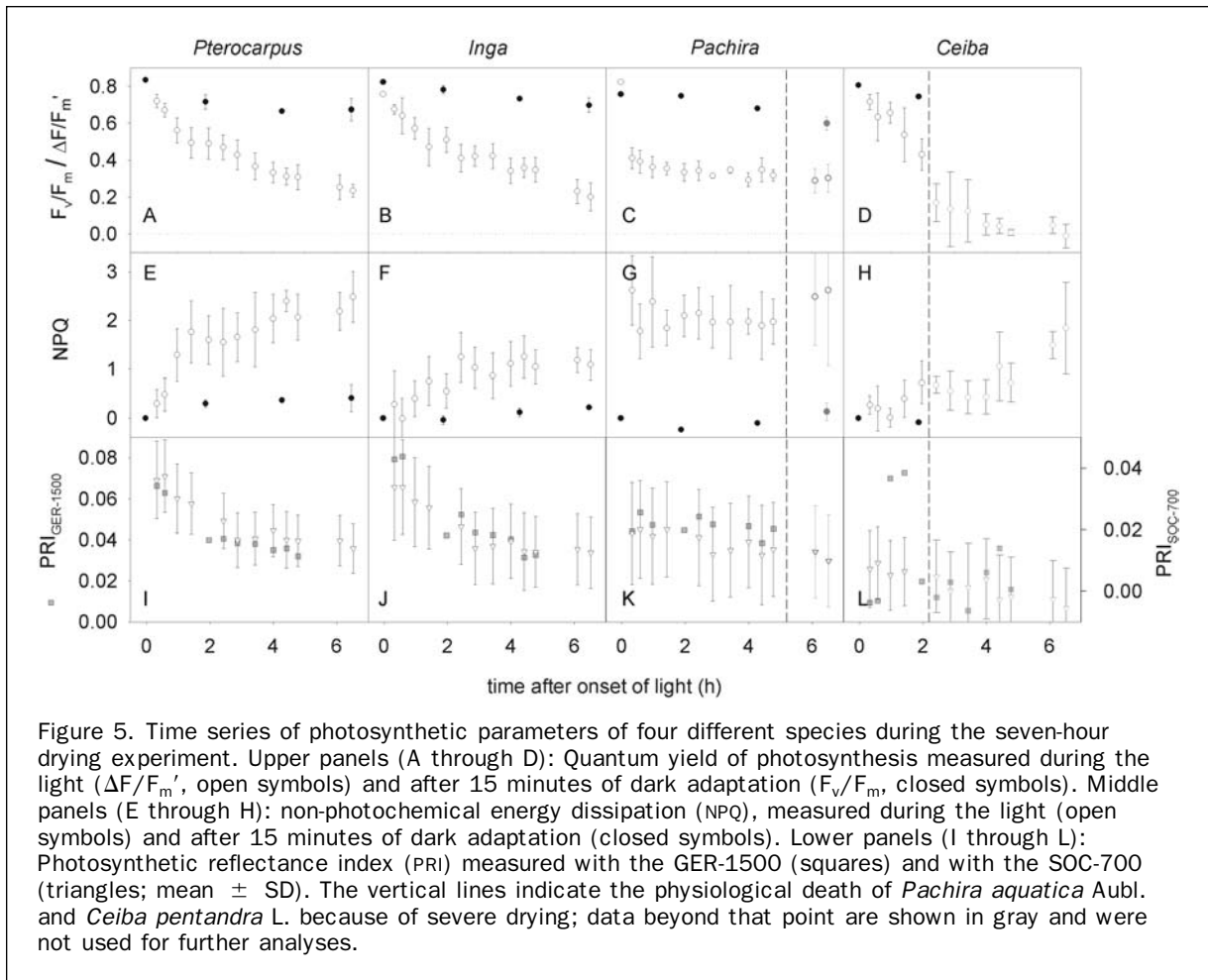


Figure 5. Time series of photosynthetic parameters of four different species during the seven-hour drying experiment. Upper panels (A through D): Quantum yield of photosynthesis measured during the light ($\Delta F/F_m'$, open symbols) and after 15 minutes of dark adaptation (F_v/F_m , closed symbols). Middle panels (E through H): non-photochemical energy dissipation (NPQ), measured during the light (open symbols) and after 15 minutes of dark adaptation (closed symbols). Lower panels (I through L): Photosynthetic reflectance index (PRI) measured with the GER-1500 (squares) and with the SOC-700 (triangles; mean \pm SD). The vertical lines indicate the physiological death of *Pachira aquatica* Aubl. and *Ceiba pentandra* L. because of severe drying; data beyond that point are shown in gray and were not used for further analyses.

TABLE 1. SPEARMAN RANK-COEFFICIENTS (r_s) INDICATING CORRELATION OF PHOTOSYNTHETIC QUANTUM YIELD ($\Delta F/F_m'$) AND NON-PHOTO-CHEMICAL ENERGY DISSIPATION (NPQ) AND THE PHOTOCHEMICAL REFLECTANCE INDEX OBTAINED BY THE GER-1500 ($PRI_{GER-1500}$) AND THE SOC-700 ($PRI_{SOC-700}$). HIGH VALUES OF r_s INDICATE MARGINAL (*) OR GOOD CORRELATION (**). NUMBERS OF SAMPLES ARE GIVEN IN PARENTHESIS

		$PRI_{GER-1500}$	$PRI_{SOC-700}$
<i>Pterocarpus indicus</i> Willd.	$\Delta F/F_m'$	0.97 (9)**	0.94 (12)**
	NPQ	-0.95 (9)**	-0.86 (12)**
<i>Ceiba pentandra</i> L.	$\Delta F/F_m'$	-0.50 (5)	0.00 (4)
	NPQ	0.10 (5)	0.20 (4)
<i>Pachira aquatica</i> Aubl.	$\Delta F/F_m'$	-0.07 (9)	0.67 (12)*
	NPQ	-0.20 (9)	-0.27 (12)
<i>Inga cf. sapindoides</i> Willd.	$\Delta F/F_m'$	0.75 (9)**	0.86 (12)**
	NPQ	-0.67 (9)*	-0.68 (12)*

Drought generally affects the xanthophyll cycle by increasing its de-epoxidation state (Herbinger *et al.*, 2002; Munné-Bosch and Peñuelas, 2003; Pieters *et al.*, 2003; Tambussi *et al.*, 2002; Winkel *et al.*, 2000). Recently, a second pigment cycle operating between two α -xanthophylls (lutein-epoxide cycle, interconversion of lutein to lutein-epoxide) was documented in photosynthetic tissues of the parasites dodder *Cuscuta reflexa* Roxb. (Bungard *et al.*, 1999), mistletoes *Amyema miquelii* (Lehm. Ex Miq.) Tiegh. (Matsubara *et al.*, 2001; 2003), *Quercus* species (Garcia-Plazaola *et al.*, 2002), and in the tropical *Inga* species (Matsubara *et al.*, 2005). Lutein-epoxide has been found in

many woody species (Garcia-Plazaola *et al.*, 2004), suggesting that the occurrence of the lutein-epoxide cycle could be common and conserved in some taxa (Matsubara *et al.*, 2003; Garcia-Plazaola *et al.*, 2002 and 2004). Based on the similarities in the chemical structure and the kinetics of de-epoxidation reactions in the two xanthophylls cycles, it has been proposed that the lutein-epoxide cycle could contribute to energy dissipation (Bungard *et al.*, 1999; Matsubara *et al.*, 2001; Garcia Plazaola *et al.*, 2003). It should be noted that any energy dissipation involving a pigment or cycle other than zeaxanthin will not be detected by PRI, which is only sensitive to the V-A-Z conversion. This could explain why the correlation between PRI and $\Delta F/F_m'$ and NPQ was weaker for the *Inga* species. Furthermore, synthesis of zeaxanthin does not account for 70 percent of the total NPQ in *Arabidopsis thaliana* (L.) Heynh. (Li *et al.*, 2000), indicating that the remaining 30 percent would result from other processes that do not involve zeaxanthin. Therefore, the level or correlation one might expect between a remotely sensed PRI (which is sensitive to zeaxanthin formation) and photosynthetic efficiency or NPQ might be at best around 70 percent. It remains a challenge for future experiments to detect shifts in the reflectance signature associated with zeaxanthin-independent NPQ, including the lutein-epoxide cycle.

Despite the physiological uncertainties, PRI was successfully used to estimate photosynthetic efficiency in a variety of correlation-based analyses (as outlined above). Nevertheless, PRI only relies on two wavebands and may have to be

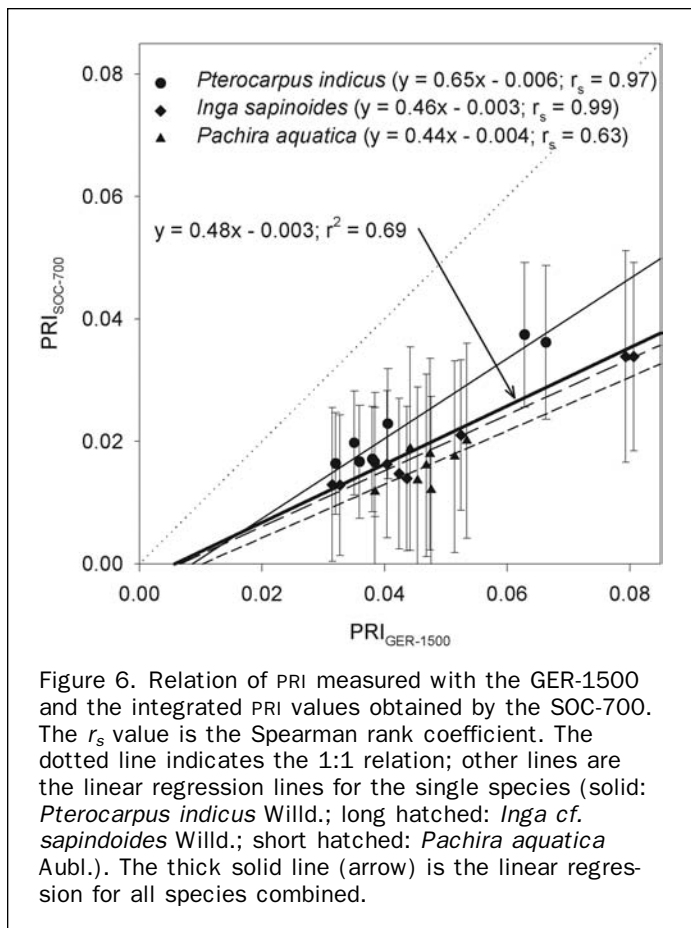


Figure 6. Relation of PRI measured with the GER-1500 and the integrated PRI values obtained by the SOC-700. The r_s value is the Spearman rank coefficient. The dotted line indicates the 1:1 relation; other lines are the linear regression lines for the single species (solid: *Pterocarpus indicus* Willd.; long hatched: *Inga cf. sapinoides* Willd.; short hatched: *Pachira aquatica* Aubl.). The thick solid line (arrow) is the linear regression for all species combined.

replaced by more sophisticated methods, which take the whole information of hyperspectral reflectance signatures into account. New methods, which could be based on spectral unmixing procedures (Asner *et al.*, 2003; Fuentes *et al.*, 2001) may quantify physiological changes of the photosynthetic apparatus more precisely than discrete indices.

Acknowledgments

We greatly thank Xiao-Ping Li and Krishna Niyogi for providing the *Arabidopsis thaliana* (L.) Heynh. mutants. We thank Marc-Thorsten Hütt for the analyses of spatial heterogeneity. We also thank Surface Optics, Inc., which provided the SOC-700 and made this survey possible. Financial support was provided by Mr. Edward Bass through a grant to Columbia University. This material is based upon work supported by the National Science Foundation under Grant No. 0340609

References

Ananyev, G., Z.S. Kolber, D. Klimov, P.G. Falkowski., J.A. Berry, U. Rascher, R. Martin, and C.B. Osmond, 2005. Remote sensing of photosynthetic efficiency, electron transport and dissipation of excess light in *Populus deltoides* stands under ambient and elevated CO₂ concentrations, and in a tropical forest canopy using a new laser-induced fluorescence transient (LIFT) device, *Global Change Biology*, 11:1195–1206.

Asner, G.P., M.M.C. Bustamante, and A.R. Townsend, 2003. Scale dependence of biophysical structure in deforested areas bordering the Tapajo's National Forest, Central Amazon, *Remote Sensing of Environment*, 87:507–520.

Barber, J., and B. Andersson, 1992. Too much of a good thing: Light can be bad for photosynthesis, *Trends in Biochemical Sciences*, 17:61–66.

Barton, C.V.M., and P.R.J. North, 2000. Remote sensing of canopy light use efficiency using the photochemical reflectance index, *Remote Sensing of Environment*, 78:264–273.

Bassi, R., and S. Caffarri, 2000. Lhc proteins and the regulation of photosynthetic light harvesting function by xanthophylls, *Photosynthesis Research*, 64:243–256.

Bilger, W., and O. Björkman, 1990. Role of the xanthophyll cycle in photoprotection elucidated by measurements of light-induced absorbance changes, fluorescence and photosynthesis in leaves of *Hedera canariensis*, *Photosynthesis Research*, 25:173–185.

Bilger, W., U. Schreiber, and M. Bock, 1995. Determination of the quantum efficiency of photosystem II and of non-photochemical quenching of chlorophyll fluorescence in the field, *Oecologia*, 102:425–432.

Bradbury, M., and N.R. Baker, 1981. Analysis of the slow phase of the chlorophyll fluorescence induction curve. Changes in the redox state of photosystem II electron acceptors and fluorescence emission from photosystem I and II, *Biochimica Biophysica Acta*, 635:542–551.

Bungard, R.A., A.V. Ruban, J.M. Hibberd, M.C. Press, P. Horton, and J.D. Scholes, 1999. Unusual carotenoids composition and a new type of xanthophyll cycle in plants, *Proceedings of the National Academy of Science, USA*, 96:1135–113.

Carter G.A., and A.K. Knapp, 2001. Leaf optical properties in higher plants: linking spectral characteristics to stress and chlorophyll concentration, *American Journal of Botany*, 88:677–684.

Carter, G.A., J.H. Jones, R.J. Mitchell, and C.H. Brewer, 1996. Detection of solar-excited chlorophyll a fluorescence and leaf photosynthetic capacity using a Fraunhofer line radiometer, *Remote Sensing of Environment*, 55:89–92.

Chaerle, L., and D. Van der Straeten, 2001. Seeing is believing: Imaging techniques to monitor plant health, *Biochimica et Biophysica Acta – Gene structure and expression*, 1519: 153–166.

Demmig, B., K. Winter, A. Krüger, and F.C. Czygan, 1987. Photoinhibition and zeaxanthin formation in intact leaves: A possible role of the xanthophyll cycle in the dissipation of excess light energy, *Plant Physiology*, 84:218–224.

Demmig-Adams, B., and W.W. Adams III, 1992. Photoprotection and other responses of plants to high light stress, *Annual Review of Plant Physiology and Plant Molecular Biology*, 43:599–626.

Enquist, B.J., E.P. Economo, T.E. Huxman, A.P. Allen, D.D. Ignace, and J.F. Gillooly, 2003. Scaling metabolism from organisms to ecosystems, *Nature*, 423:639–642.

Filella, I., J.L. Amaro, J.L. Araus, and J. Peñuelas, 1996. Relationship between photosynthetic radiation use efficiency of barley canopies and the photochemical reflectance index (PRI), *Physiologia Plantarum*, 96:211–216.

Filella I., J. Peñuelas, L. Llorens, and M. Estiarte, 2004. Reflectance assessment of seasonal and annual changes in biomass and CO₂ uptake of a Mediterranean shrubland submitted to experimental warming and drought, *Remote Sensing of Environment*, 90: 308–318.

Frak, E., X. Le Roux, P. Millard, B. Adam, E. Dreyer, C. Escuit, H. Sinoquet, M. Vandame, and C. Varlet-Grancher, 2002. Spatial distribution of leaf nitrogen and photosynthetic capacity within the foliage of individual trees: Disentangling the effects of local light quality, leaf irradiance, and transpiration, *Journal of Experimental Botany*, 53:2207–2216.

Fuentes D.A., J.A. Gamon, H.L. Qiu, D.A. Sims, and D.A. Roberts, 2001. Mapping Canadian boreal forest vegetation using pigment and water absorption features derived from the AVIRIS sensor, *Journal of Geophysical Research – Atmospheres*, 106: 33565–33577.

Gamon, J.A., I. Filella, and J. Peñuelas, 1993. The dynamic 531-nm Δ reflectance signal: A survey of 20 angiosperm species, *Photosynthetic Responses to the Environment* (H.Y. Yamamoto and C.M. Smith, editors), American Society of Plant Physiologists, Rockville, Maryland, pp. 172–177.

Gamon, J.A., J. Peñuelas, and C.B. Field, 1992. A narrow-waveband spectral index that tracks diurnal changes in photosynthetic efficiency, *Remote Sensing of Environment*, 41:35–44.

- Gamon, J.A., L. Serrano, and J.S. Surfus, 1997. The photochemical reflectance index: An optical indicator of photosynthetic radiation use efficiency across species, functional types and nutrient levels, *Oecologia*, 112:492–501.
- García-Plazaola, J.I., A. Hernández, E. Errasti, and J.M. Becerril, 2002. Occurrence and operation of the lutein-epoxide cycle in *Quercus* species, *Functional Plant Biology*, 29:1075–1080.
- García-Plazaola, J.I., K. Hormaetxe, A. Hernández, J.M. Olano, and J.M. Becerril, 2004. The lutein epoxide cycle in vegetative buds of woody plants, *Functional Plant Biology*, 31:815–823.
- Genty, B., J.M. Briantais, and N.R. Baker, 1989. The relationship between the quantum yield of photosynthetic electron transport and quenching of chlorophyll fluorescence, *Biochimica Biophysica Acta*, 990:87–92.
- Green, A.A., M. Berman, P. Switzer, and M.D. Craig, 1988. A transformation for ordering multispectral data in terms of image quality with implications for noise removal, *IEEE Transactions on Geoscience and Remote Sensing*, 26:65–74.
- Grieu, P., C. Robin, and A. Guckert, 1995. Effect of drought on photosynthesis in *Trifolium repens*: Maintenance of photosystem II efficiency photosynthesis, *Plant Physiology and Biochemistry*, 33:19–24.
- Guo, J., and C.M. Trotter, 2004. Estimating photosynthetic light-use efficiency using the photochemical reflectance index: Variations among species, *Functional Plant Biology*, 31:255–265.
- Herbinger, K., M. Tausz, A. Wonisch, G. Soja, A. Sorger, and D. Grill, 2002. Complex interactive effects of drought and ozone stress on the antioxidant defense systems of two wheat cultivars, *Plant Physiology and Biochemistry*, 40:691–696.
- Horton, P., A.V. Ruben, and R.G. Walters, 1996. Regulation of light harvesting in green plants, *Annual Reviews of Plant Physiology and Plant Molecular Biology*, 47:655–684.
- Hütt, M.-T., and R. Neff, 2001. Quantification of spatiotemporal phenomena by means of cellular automata techniques, *Physica A*, 289:498–516.
- Kolber, Z.S., O. Prasil, and P.G. Falkowski, 1998. Measurements of variable chlorophyll fluorescence using fast repetition rate techniques: Defining methodology and experimental protocols, *Biochimica Biophysica Acta – Bioenergetics*, 1367: 88–106.
- Kolber, Z.S., D. Klimov, G. Ananyev, U. Rascher, J.A. Berry, and C.B. Osmond, 2005. Measuring photosynthetic parameters at a distance: laser induced fluorescence transient (LIFT) method for remote measurements of PSII in terrestrial vegetation, *Photosynthesis Research*, 84:121–129.
- Krause, G.H., and E. Weis, 1991. Chlorophyll fluorescence and photosynthesis: The basics, *Annual Review of Plant Physiology and Plant Molecular Biology*, 42:313–349.
- Li, X.P., O. Björkman, C. Shih, A.R. Grossman, M. Rosenquist, S. Jansson, and K.A. Niyogi, 2000. Pigment-binding protein essential for regulation of photosynthetic light harvesting, *Nature*, 403:391–395.
- Li, X.P., P. Müller-Moulé, A.M. Gilmore, and K.K. Niogi, 2002. PsbS-dependent enhancement of feedback de-excitation protects photosystem II from photoinhibition, *Proceedings National Academy Science*, 99:15222–15227.
- Matsubara, S., A.M. Gilmore, and C.B. Osmond, 2001. Diurnal and acclimatory responses of violaxanthin and lutein epoxide in the Australian mistletoe *Amyema miquelii*, *Australian Journal of Plant Physiology*, 28:793–800.
- Matsubara, S., T. Morosinotto, R. Bassi, A.L. Christian, E. Fischer-Schliebs, U. Lüttge, B. Orthen, A.C. Franco, F.R. Scarano, B. Förster, B.J. Pogson, and C.B. Osmond, 2003. Occurrence of the lutein epoxide cycle in mistletoes of Loranthaceae and Viscaceae, *Planta*, 217:868–879.
- Matsubara S., M. Naumann, R. Martin, C.J. Nichol, U. Rascher, T. Morosinotto, R. Bassi, and C.B. Osmond, 2005. Slowly reversible de-epoxidation of lutein-epoxide in deep shade leaves of a tropical tree legume may 'lock-in' lutein-based photoprotection during acclimation to strong light, *Journal of Experimental Botany*, 56:461–468.
- Maxwell, K., and G.N. Johnson, 2000. Chlorophyll fluorescence – A practical guide, *Journal of Experimental Botany*, 51:659–668.
- Methy, M., 2000. Analysis of photosynthetic activity at the leaf and canopy levels from reflectance measurements: A case study, *Photosynthetica*, 38:505–512.
- Meyer, S., and B. Genty, 1998. Mapping intercellular CO₂ mole fraction (C-i) in *Rosa rubiginosa* leaves fed with abscisic acid by using chlorophyll fluorescence imaging – Significance of C-i estimated from leaf gas exchange, *Plant Physiology*, 116: 947–957.
- Meyer, S., and B. Genty, 1999. Heterogeneous inhibition of photosynthesis over the leaf surface of *Rosa rubiginosa* L. during water stress and abscisic acid treatment: Induction of a metabolic component by limitation of CO₂ diffusion, *Planta*, 210:126–131.
- Munné-Bosch, S., and J. Peñuelas, 2003. Photo- and antioxidative protection, and a role for salicylic acid during drought and recovery in field-grown *Phillyrea angustifolia* plants, *Planta*, 217:758–766.
- National Academies, 2004. *Implementing Climate and Global Change Research: A Review of the Final U.S. Climate Change Science Program Strategic Plan*, The National Academy Press, Washington, D.C., 152 p.
- Nichol, C.J., K.F. Hümmrich, T.A. Black, P.G. Jarvis, C.L. Walthall, J. Grace, and F.G. Hall, 2000. Remote sensing of photosynthetic-light-use efficiency of boreal forest, *Agricultural and Forest Meteorology*, 101:131–142.
- Nichol, C.J., J. Lloyd, O. Shibistova, A. Arneth, C. Roser, A. Knohl, S. Matsubara, and J. Grace, 2002. Remote sensing of photosynthetic light use efficiency of Siberian boreal forest, *Tellus B*, 54:677–687.
- Osmond, C.B., P.F. Daley, M.R. Badger, and U. Lüttge, 1998. Chlorophyll fluorescence quenching during photosynthetic induction in leaves of *Abutilon striatum* Dicks. infected with Abutilon mosaic virus, observed with a field-portable imaging system, *Botanica Acta*, 111:390–397.
- Osmond, C.B., D. Kramer, and U. Lüttge, 1999. Reversible, water stress-induced non-uniform chlorophyll fluorescence quenching in wilting leaves of *Potentilla reptans* may not be due to patchy stomatal responses, *Plant Biology*, 1:618–624.
- Osmond, C.B., and Y.-M. Park, 2001. Field-portable imaging systems for measurement of chlorophyll fluorescence quenching, *Air Pollution and Plant Biotechnology – Prospects for Phytomonitoring and Phytoremediation* (K. Omasa, H. Saji, S. Youssefian, and N. Kondo, editors), Springer, Tokyo.
- Peñuelas, J., F. Baret, and I. Filella, 1995a. Semi-empirical indices to assess carotenoid/chlorophyll a ratio from leaf spectral reflectance, *Photosynthetica*, 31:221–230.
- Peñuelas, J., I. Filella, and J.A. Gamon, 1995b. Assessment of photosynthetic radiation-use efficiency with spectral reflectance, *New Phytologist*, 131:291–296.
- Peñuelas, J., and Y. Inoue, 2000. Reflectance assessment of canopy CO₂ uptake, *International Journal of Remote Sensing*, 21: 3353–3356.
- Peñuelas, J., J. Llusia, J. Pinol, and I. Filella, 1997. Photochemical reflectance index and leaf radiation-use efficiency assessment in Mediterranean trees, *International Journal of Remote Sensing*, 13:2863–2868.
- Pieters, A.J., W. Tezara, and A. Herrera, 2003. Operation of the xanthophyll cycle and degradation of D1 protein in the inducible CAM plant, *Talinum triangulare*, under water deficit, *Annals of Botany*, 92:393–399.
- Rahman, A.F., J.A. Gamon, D.A. Fuentes, and D. Prentiss, 2001. Modelling spatially distributed ecosystem flux of boreal forest using hyper-spectral indices from AVIRIS imagery, *Journal of Geophysical Research*, 106 (D24):33579–33591.
- Rascher, U., 2003. Imaging and imagining spatiotemporal variations of photosynthesis on simple leaves, *Nonlinear Dynamics and the Spatiotemporal Principles of Biology* (F. Beck, M.-T. Hütt and U. Lüttge, editors.), *Nova Acta Leopoldina*, 88:367–380.
- Rascher, U., and U. Lüttge, 2002. High-resolution chlorophyll fluorescence imaging serves as a non-invasive indicator to monitor the spatio-temporal variations of metabolism during the day-night cycle and during the endogenous rhythm in continuous light in the CAM-plant *Kalanchoë daigremontiana*, *Plant Biology*, 4:671–681.

- Rascher, U., E.G. Bobich, G.H. Lin, A. Walter, T. Morris, M. Naumann, C.J. Nichol, D. Pierce, K. Bil, V. Kudryarov, and J.A. Berry, 2004. Functional diversity of photosynthesis during drought in a model tropical rainforest – The contributions of leaf area, photosynthetic electron transport and stomatal conductance to reduction in net ecosystem carbon exchange, *Plant, Cell & Environment*, 27:1239–1256.
- Rascher, U., M.-T. Hütt, K. Siebke, C.B. Osmond, F. Beck, and U. Lüttge, 2001. Spatio-temporal variations of metabolism in a plant circadian rhythm: The biological clock as an assembly of coupled individual oscillators, *Proceedings of the National Academy of Science USA*, 98:11801–11805.
- Research Systems Inc., 2000. *ENVI 3.4 Users Manual*, Boulder, Colorado.
- Richardson, A.D., and G.P. Berlyn, 2002. Changes in foliar spectral reflectance and chlorophyll fluorescence of four temperate species following branch cutting, *Tree Physiology*, 22:499–506.
- Schreiber, U., and W. Bilger, 1993. Progress in chlorophyll fluorescence research: Major developments during the past years in retrospect, *Proceedings of Botany*, 53:151–173.
- Schreiber, U., W. Bilger, and C. Neubauer, 1995. Chlorophyll fluorescence as a noninvasive indicator for rapid assessment of in vivo photosynthesis, *Ecophysiology of photosynthesis* (E.D. Schulze and M.M. Caldwell, editors), Springer, Berlin, Heidelberg, New York, pp. 49–70.
- Schulze, E.D., and M.M. Caldwell, editors, 1995. *Ecophysiology of photosynthesis. Ecological Studies, Vol. 100*, Springer, Berlin, Heidelberg, New York, 576 p.
- Stylinski, C.D., J.A. Gamon, and W.C. Oechel, 2002. Seasonal patterns of reflectance indices, carotenoid pigments and photosynthesis of evergreen chaparral species, *Oecologia*, 131:366–374.
- Tambussi, E.A., J. Casadesus, S.M. Munné-Bosch, and J.L. Araus, 2002. Photoprotection in water-stressed plants of durum wheat (*Triticum turgidum* var. *durum*): Changes in chlorophyll fluorescence, spectral signature and photosynthetic pigments, *Functional Plant Biology*, 29:35–44.
- Thornley, J.H.M., 1998. Dynamic model of leaf photosynthesis with acclimation to light and nitrogen, *Annals of Botany*, 81:421–430.
- Trotter, G.M., D. Whitehead, and E.J. Pinkney, 2002. The photochemical reflectance index as a measure of photosynthetic light use efficiency for plants with varying foliar nitrogen content, *International Journal of Remote Sensing*, 23:1207–1212.
- Valentini, R., D. Epron, P. DeAngelis, G. Matteucci, and E. Dreyer, 1995. In situ estimation of net CO₂ assimilation, photosynthetic electron flow and photorespiration in Turkey oak (*Q. cerris* L.) leaves: Diurnal cycles under different levels of water supply, *Plant Cell Environment*, 18:631–640.
- Walter A., U. Rascher, and C.B. Osmond, 2004. Transition in photosynthetic parameters of midvein and interveinal regions of leaves and their importance during leaf growth and development, *Plant Biology*, 6:184–191.
- Winkel, T., M. Méthy, and F. Thénot, 2000. Radiation use efficiency, chlorophyll fluorescence, and reflectance indices associated with ontogenic changes in water-limited *Chenopodium quinoa*, *Photosynthetica*, 40:227–232.

(Received 19 May 2005; accepted 15 August 2005; revised 23 September 2005)